Title	The Benard Problem of Rarefied Gas Dynamics(Mathematical Fluid Mechanics and Modeling)
Author(s)	Sone, Yoshio; Aoki, Kazuo; Sugimoto, Hiroshi; Motohashi, Hideto
Citation	数理解析研究所講究録 (1994), 888: 145-157
Issue Date	1994-10
URL	http://hdl.handle.net/2433/84342
Right	
Type	Departmental Bulletin Paper
Textversion	publisher

数理解析研究所講究録
第888巻 1994年 145-157

The Bénard Problem of Rarefied Gas Dynamics

Yoshio Sone, Kazuo Aoki, Hiroshi Sugimoto, and Hideto Motohashi

（曾根良夫，青木一生，杉元　宏，本橋秀人）

Division of Aeronautics and Astronautics,

Graduate School of Engineering, Kyoto University,

Kyoto 606-01, Japan

Abstract

The two-dimensional Bénard problem of a rarefied gas in a rectangular domain is studied numerically by a finite-difference analysis of the Boltzmann-Krook-Welander equation. The diffuse reflection is assumed on the upper cooled wall and on the lower heated wall and the specular reflection on the side boundaries. The range of the parameters where a convection exists, steady flow patterns, a bifurcation of flow pattern, and a process of convergence to an array of uniform size rolls are presented.

I. Introduction

The Bénard problem concerning the instability of a layer of fluid heated from below has long been of interest to many scientists and engineers, and a lot of works have been done on the basis of the continuum theory[1-5]. The study of the problem of a rarefied gas is just at a starting point, and only a few works[6], which their authors call preliminary, have been done by the direct simulation Monte Carlo method[7,8]. In a series of papers we will study the problem more systematically and try to obtain more comprehensive result of the problem. In the present paper we consider the two-dimensional Bénard problem of a rarefied gas in a rectangular domain and investigate the condition (the range of the parameters included in the problem) that allows a state with flow, flow patterns, and bifurcation of

flow. Numerical analysis by a finite-difference method on the basis of the Boltzmann-Krook-Welander equation[8–10] is chosen to pursue the problem.

II. Problem and basic equation

In this paper we consider two dimensional flows of a rarefied gas in a rectangular domain ($0 < X_1 < L$, $0 < X_2 < D$; X_i is the Cartesian coordinate system), where the gas is subject to a uniform gravitational force in the negative X_2 direction, the lower boundary at $X_2 = 0$ is heated at a uniform temperature T_h, and the upper at $X_2 = D$ is cooled at a uniform temperature T_c. We analyze the behavior of the gas under the following assumptions:

i) The behavior of the gas is described by the Boltzmann-Krook-Welander equation.

ii) The molecules make the diffuse reflection on the upper and lower boundaries.

iii) The molecules make the specular reflection on the side boundaries at $X_1 = 0$ and L.

The Boltzmann-Krook-Welander equation is given by

$$\frac{\partial f}{\partial t} + \xi_1 \frac{\partial f}{\partial X_1} + \xi_2 \frac{\partial f}{\partial X_2} - g \frac{\partial f}{\partial \xi_2} = A_c \rho (f_e - f), \tag{1}$$

$$f_e = \frac{\rho}{(2\pi RT)^{3/2}} \exp\left(-\frac{(\xi_i - v_i)^2}{2RT}\right), \tag{2}$$

$$\rho = \int f \, d\xi_1 \, d\xi_2 \, d\xi_3, \tag{3a}$$

$$v_i = \rho^{-1} \int \xi_i f \, d\xi_1 \, d\xi_2 \, d\xi_3, \tag{3b}$$

$$3RT = \rho^{-1} \int (\xi_i - v_i)^2 f \, d\xi_1 \, d\xi_2 \, d\xi_3. \tag{3c}$$

Here, the notations are as follows: t is the time; ξ_i is the molecular velocity; f is the velocity distribution function; ρ is the density of the gas; v_i is the flow velocity ($v_3 = 0$) of the gas; T is the temperature of the gas; g is the acceleration of gravity; A_c is a constant ($A_c\rho$ is the collision frequency of a molecule, which is common to all the molecules in the case of the Boltzmann-Krook-Welander model); R is the specific gas constant. The integrals in Eqs. (3a)–(3c) are carried out over the whole ξ_i space.

The boundary conditions on the upper and lower boundaries are, at $X_2 = 0$,

$$f = \rho_h(2\pi RT_h)^{-3/2}\exp(-\xi_i^2/2RT_h), \qquad (\xi_2 > 0), \tag{4a}$$

$$\rho_h = -(2\pi/RT_h)^{1/2}\int_{\xi_2<0}\xi_2 f\,d\xi_1\,d\xi_2\,d\xi_3, \tag{4b}$$

and, at $X_2 = D$,

$$f = \rho_c(2\pi RT_c)^{-3/2}\exp(-\xi_i^2/2RT_c), \qquad (\xi_2 < 0), \tag{5a}$$

$$\rho_c = (2\pi/RT_c)^{1/2}\int_{\xi_2>0}\xi_2 f\,d\xi_1\,d\xi_2\,d\xi_3. \tag{5b}$$

The boundary conditions on the side boundaries are, at $X_1 = 0$,

$$f(X_1, X_2, t, \xi_1, \xi_2, \xi_3) = f(X_1, X_2, t, -\xi_1, \xi_2, \xi_3), \qquad (\xi_1 > 0), \tag{6}$$

and, at $X_1 = L$,

$$f(X_1, X_2, t, \xi_1, \xi_2, \xi_3) = f(X_1, X_2, t, -\xi_1, \xi_2, \xi_3), \qquad (\xi_1 < 0). \tag{7}$$

The initial condition is, at $t = 0$,

$$f = f_0, \tag{8}$$

where f_0 is properly chosen.

By use of properly chosen nondimensional variables, Eqs. (1)–(3c) and the boundary conditions (4a)–(7) are reduced to a system characterized by the four parameters: the Knudsen number $Kn[= (8RT_0/\pi)^{1/2}(A_c\rho_0)^{-1}D^{-1} = \ell_0/D]$, the Froude number $Fr(= 2RT_h/Dg)$, the temperature ratio T_c/T_h, and the aspect ratio L/D, where ρ_0 is the average density of the gas over the domain, ℓ_0 is the mean free path of the state f_e [in Eq. (2)] with $\rho = \rho_0$, $T = T_h$, and $v_i = 0$.

Equations (1)–(3c) with the boundary condition (4a)–(7) has a time-independent solution without flow ($v_i \equiv 0$) for any set of the parameters. Let it be $f_s(X_2, \xi_i)$ and let the corresponding density and temperature be $\rho_s(X_2)$ and $T_s(X_2)$. When the gravity is strong (when Fr is small), the density ρ_s decreases as X_2 increases, but when the gravity is weak

(when Fr is large), ρ_s increases with X_2. In the intermediate gravity (intermediate Fr), ρ_s first decreases with X_2, reaches its minimum, and then increases. Our interest is the possibility of another type of solutions with nonzero flow velocity, such as a steady solution of a convection roll, in a rarefied gas. Thus, we numerically analyze the initial and boundary-value problem (1)–(7) for many sets of parameters and investigate the range of parameters where solutions with flow exist, and their flow pattern. Further, we present an example of flow bifurcation, i.e., approach to different types of steady solutions from slightly different initial conditions.

The independent variable ξ_3 can be eliminated from the system (1)–(7), if we are satisfied with the information of the marginal distribution functions $\int_{-\infty}^{\infty} f d\xi_3$ and $\int_{-\infty}^{\infty} \xi_3^2 f d\xi_3$. The system for these quantities is obtained by integrating Eq. (1), (4a), (5a), (6), and (7) multiplied by 1 or ξ_3^2 with respect to ξ_3 over $(-\infty < \xi_3 < \infty)$. In the present work, we carry out a standard finite-difference numerical analysis of this system.

III. Existence range of nonstationary solutions and their flow patterns

In order to find the range of the parameters (Fr, T_c/T_h, etc.) where a flow occurs in the rectangular domain, we investigate the initial and boundary-value problem (1)–(7) for many sets of the parameters and pursue the long-time behavior of the solution. As the initial distribution function f_0 in Eq. (8), we take the Maxwellian distribution:

$$\begin{aligned} f_0 &= \rho(2\pi RT)^{-3/2}\exp(-\xi_i^2/2RT), \\ \rho &= \rho_s(X_2), \qquad T = T_s(X_2)[1 + (1/2)\cos(\pi X_1/L)\sin(\pi X_2/D)], \end{aligned} \tag{9}$$

where $\rho_s(X_2)$ and $T_s(X_2)$ are the density and temperature of the stationary solution for the corresponding values of the parameters. (It is noted that the Maxwellian distribution with ρ_s and T_s is not the solution of Eq. (1) owing to its gravitational term.)

Pursuing the long-time behavior of the solution of the initial and boundary-value problem (1)–(7), we find that the solution approaches the corresponding stationary solution f_s or a steady solution consisting of a single convection roll for all the cases computed. The

parameter range of the two class of solutions is shown in Figs. 1–3, where the stationary solution is marked by • and the steady solution of a convection roll by ○ in the (Fr, T_c/T_h) plane. Fig. 1 is the result at $Kn = 0.02$, 0.03, 0.04, 0.05, and 0.06 in the square domain $L/D = 1$, Fig. 2 is the result at $Kn = 0.02$ in the domain $L/D = 3/4$, and Fig. 3 is the result at $Kn = 0.02$ in the domain $L/D = 1/2$. A steady convection roll of flow exists in a triangular region in the (Fr, T_c/T_h) plane, and it rapidly shrinks as the Knudsen number increases. According to the linear stability analysis[5] based on the continuum theory, $Ra \doteq 1700$, where $Ra = (16/\pi)(1 - T_c/T_h)/(T_c/T_h)FrKn^2$ (Rayleigh number), is the critical value above which the stationary solution is unstable. In Fig. 1 the curve $Ra = 1700$ is shown by a dashed line. As mentioned in Sec. II, the density $\rho_s(X_2)$ of a stationary solution decreases monotonically as X_2 increases for small Fr, but has its minimum in the gas for intermediate Fr. The approximate boundary of these regions is shown by a chain line in Fig. 1.

The computation is carried out only for a special initial condition. Thus, in the triangular region with ○ sign, a single roll of steady flow certainly exists, but another type of flow may occur. In fact we will show such examples, besides the reversal $f(L - X_1, X_2, -\xi_1, \xi_2, \xi_3)$ of a solution $f(X_1, X_2, \xi_1, \xi_2, \xi_3)$, in Sec. IV. In the region with • sign, the existence of a flow cannot be excluded, but various tests, although they are not systematic but are randomly carried out, show that occurrence of a perpetual flow is improbable.

Example of flow fields (flow velocity vectors, isodensity lines, and isothermal lines) in the case of $L/D = 1$ are shown in Figs. 4 and 5. In Fig. 4 the results at $Kn = 0.02$ and $T_c/T_h = 0.4$ are shown for three typical Froude numbers $Fr = 2$, 3, and 7.5, which correspond to three different types of $\rho_s(X_2)$ mentioned in Sec. II. In Fig. 5 the results for two different Knudsen numbers, $Kn = 0.02$ and 0.04 with the other parameters being common ($T_c/T_h = 0.1$, $Fr = 3$) are shown. The lateral position of the center of the roll is nearly at $X_1 = 2L/3$ for all the cases in Figs. 4 and 5, but its vertical position differs appreciably depending on the parameters.

IV. Array of rolls and bifurcation of flow

A steady solution of Eq. (1) extended across a specularly reflecting plane boundary by joining its mirror image or reversal (i.e. extended symmetrically with respect to the boundary) can be shown to be a solution of Eq. (1) in a wider domain. Thus, by arranging a series of steady solutions of a kind laterally in such a way that adjacent solutions are the mirror images of each other, we can construct a steady solution in a wider domain. The array f_a^N of N steady solutions of a single roll f_a in the domain with $L/D = a$ so arranged forms a solution consisting of N rolls in the domain $L/D = Na$. For example both $f_{3/4}^4$ and f_1^3 are solutions in the domain $L/D = 3$.

Our next interest is bifurcation to these different types of flow. Taking, as the initial condition f_0 in the initial and boundary value problem (1)–(7) in the domain $L/D = k\ell/m$,

$$f_0 = \alpha f_{k/m}^{\ell} + (1-\alpha) f_{\ell/m}^{k} \ , \tag{10}$$

where α is a constant ($0 \leq \alpha \leq 1$) and k, ℓ, and m are positive integers, we pursue the time-development of the solution and investigate the type of the limiting solution as $t \to \infty$ for different α.

Here we give some results in the domain $L/D = 3$ for the initial condition (10) with $\ell = 4$, $k = 3$, and $m = 4$ for $Fr = 3$ and $T_c/T_h = 0.1$. When $Kn = 0.02$, the solution approaches f_1^3 for $\alpha = 0.6$ but $f_{3/4}^4$ for $\alpha = 0.7$; when $Kn = 0.03$, it approaches f_1^3 for $\alpha = 0.8$ but $f_{3/4}^4$ for $\alpha = 0.9$; when $Kn = 0.04$, even for $\alpha = 0.99$, it approaches f_1^3. Several tests indicate that if $f \to f_{3/4}^4$ for α_1, then $f \to f_{3/4}^4$ for $\alpha \geq \alpha_1$ and that if $f \to f_1^3$ for α_2, then $f \to f_1^3$ for $\alpha \leq \alpha_2$. The transition processes for $\alpha = 0.6$ and 0.7 at $Kn = 0.02$ are shown in Fig. 6.

References

1. Bénard, H. (1900): Les tourbillons cellulaires dans une nappe liquide. *Revue Gén. Sci. Pur. Appl.*, **11**, 1261-1271, 1309-1328.

2. Rayleigh, L. (1916): On convection currents in a horizontal layer of fluid when the higher temperature is on the under side. *Phil. Mag.*, **32**, 529-546.

3. Busse, F. H. and Clever, R. M. (1979): Instabilities of convection rolls in a fluid of moderate Prandtl number. *J. Fluid Mech.*, **91**, 319-335.

4. Mizushima, J. and Fujimura, K. (1992): Higher harmonic resonance of two-dimensional distributions in Rayleigh-Bénard convection. *J. Fluid Mech.*, **234**, 651-667.

5. Koschmieder, E. L. (1993): *Bénard Cells and Taylor Vortices.* Cambridge Univ. Press, Cambridge.

6. Cercignani, C. and Stefanov, S. (1992): Bénard's instability in kinetic theory. *Transp. Theory Stat. Phys.*, **21**, 371-381; Stefanov, S. and Cercignani, C. (1992): Monte Carlo simulation of Bénard's instability in a rarefied gas. *Eur. J. Mech., B/Fluids*, **11**, 543-554.

7. Bird, G. A. (1976): *Molecular Gas Dynamics.* Clarendon Press, Oxford.

8. Sone, Y. and Aoki, K. (1994): *Molecular Gas Dynamics* (Appendix II). Asakura, Tokyo.

9. Bhatnagar, P. L., Gross, E. P. and Krook, M. (1954): A model for collision processes in gases, I. *Phys. Rev.*, **94**, 511-525.

10. Welander, P. (1954): On the temperature jump in a rarefied gas. *Ark. Fys.* **7**, 507-553.

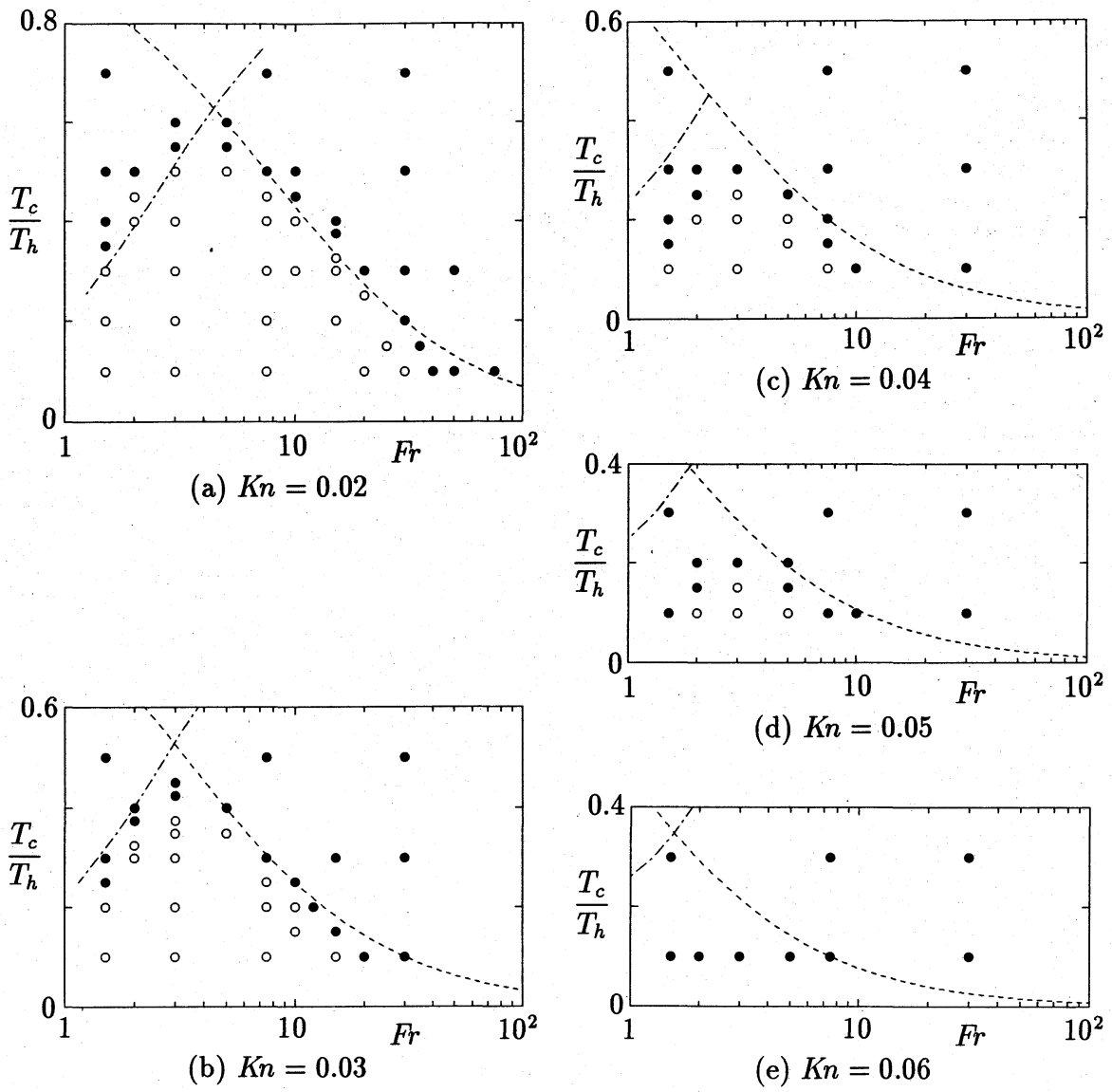

Fig. 1. The range of the parameters Fr and T_c/T_h where a convection roll exists for $L/D = 1$. (a) $Kn = 0.02$, (b) $Kn = 0.03$, (c) $Kn = 0.04$, (d) $Kn = 0.05$, and (e) $Kn = 0.06$. o : Convection occurs; • : No flow occurs. See the second paragraph in Sec. III for ---- and -·-·- . [The (X_1, X_2) space is divided into 24×24 nonuniform rectangular lattices finer near the upper and right boundaries. The (ξ_1, ξ_2) space, limited to $|\xi_1|$ and $|\xi_2| \leq 4(2RT_h)^{1/2}$, is divided into 40×40 nonuniform rectangular lattices, finer near the lines $\xi_1 = 0$ and $\xi_2 = 0$.]

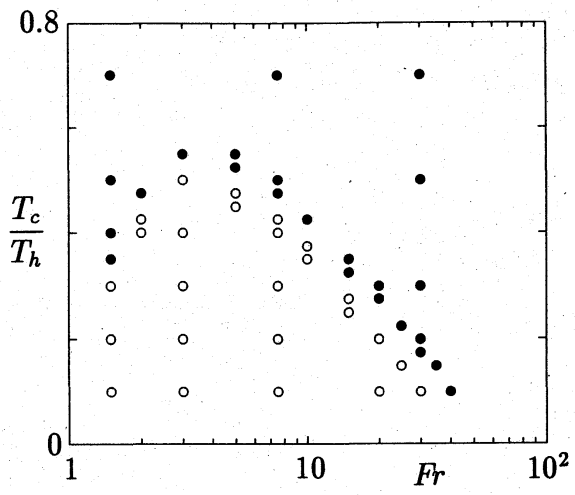

Fig. 2. The range of the parameters Fr and T_c/T_h where a convection roll exists for $L/D = 3/4$ and $Kn = 0.02$. o : Convection occurs; • : No flow occurs. (See the caption of Fig. 1 for the lattice system.)

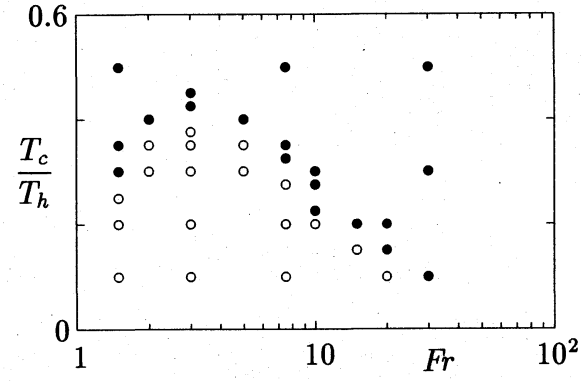

Fig. 3. The range of the parameters Fr and T_c/T_h where a convection roll exists for $L/D = 1/2$ and $Kn = 0.02$. o : Convection occurs; • : No flow occurs. (See the caption of Fig. 1 for the lattice system.)

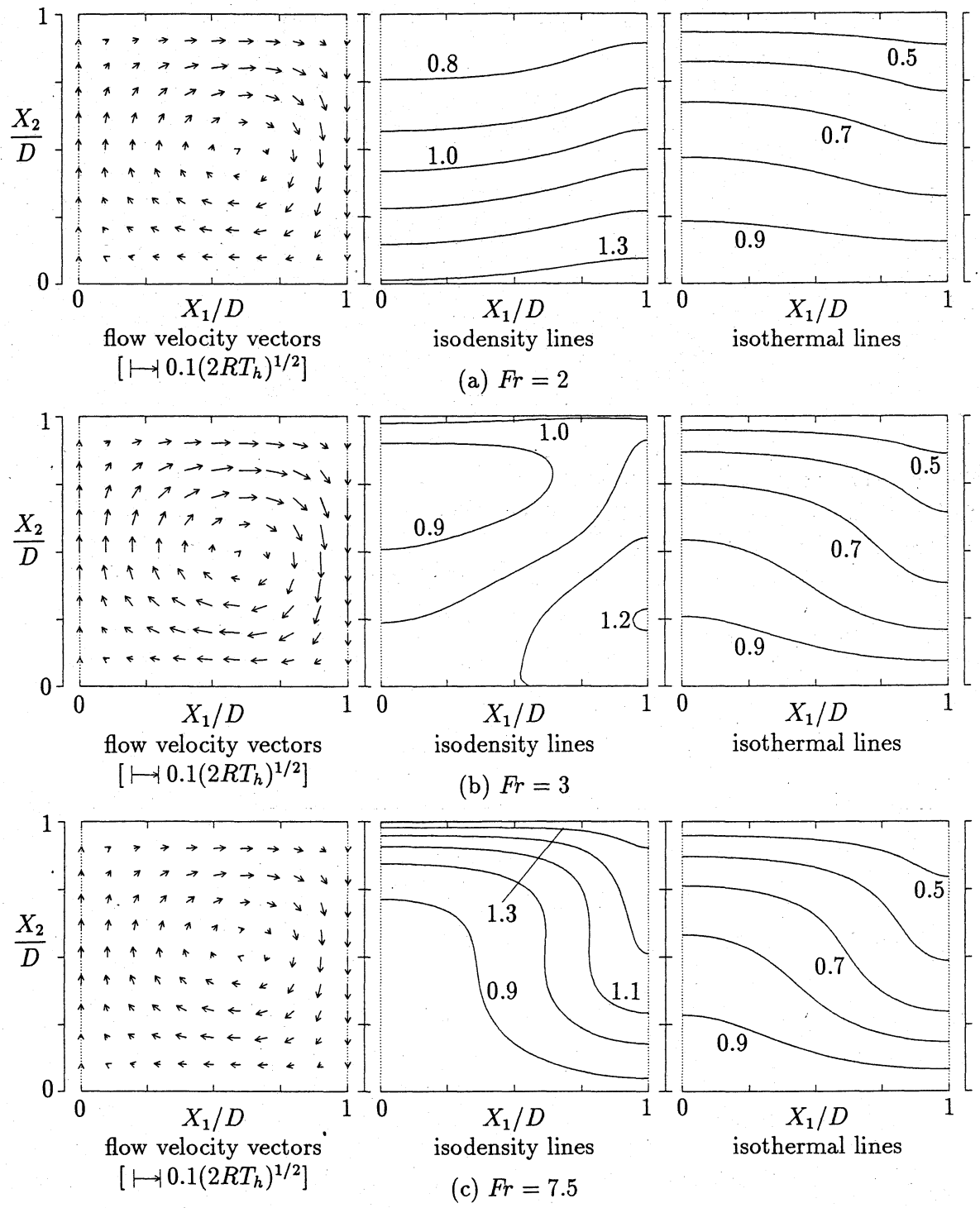

Fig. 4. Flow velocity vectors, isodensity lines, and isothermal lines for three Froude numbers, $Fr = 2$, 3, and 7.5, with $L/D = 1$, $Kn = 0.02$, and $T_c/T_h = 0.4$. (a) $Fr = 2$, (b) $Fr = 3$, and (c) $Fr = 7.5$. The arrows indicate the velocity at their starting points. The contours $\rho/\rho_0 = 0.1n$ and $T/T_h = 0.1n$ are shown. [The (X_1, X_2) space is divided into 48×48 [in (a) and (b)] or 72×72 [in (c)] nonuniform rectangular lattices finer near the upper and right boundaries. The (ξ_1, ξ_2) space, limited to $|\xi_1|$ and $|\xi_2| \leq 4(2RT_h)^{1/2}$, is divided into 40×80 [in (a)], 40×60 [in (b)], or 40×40 [in (c)] nonuniform rectangular lattices, finer near the lines $\xi_1 = 0$ and $\xi_2 = 0$.]

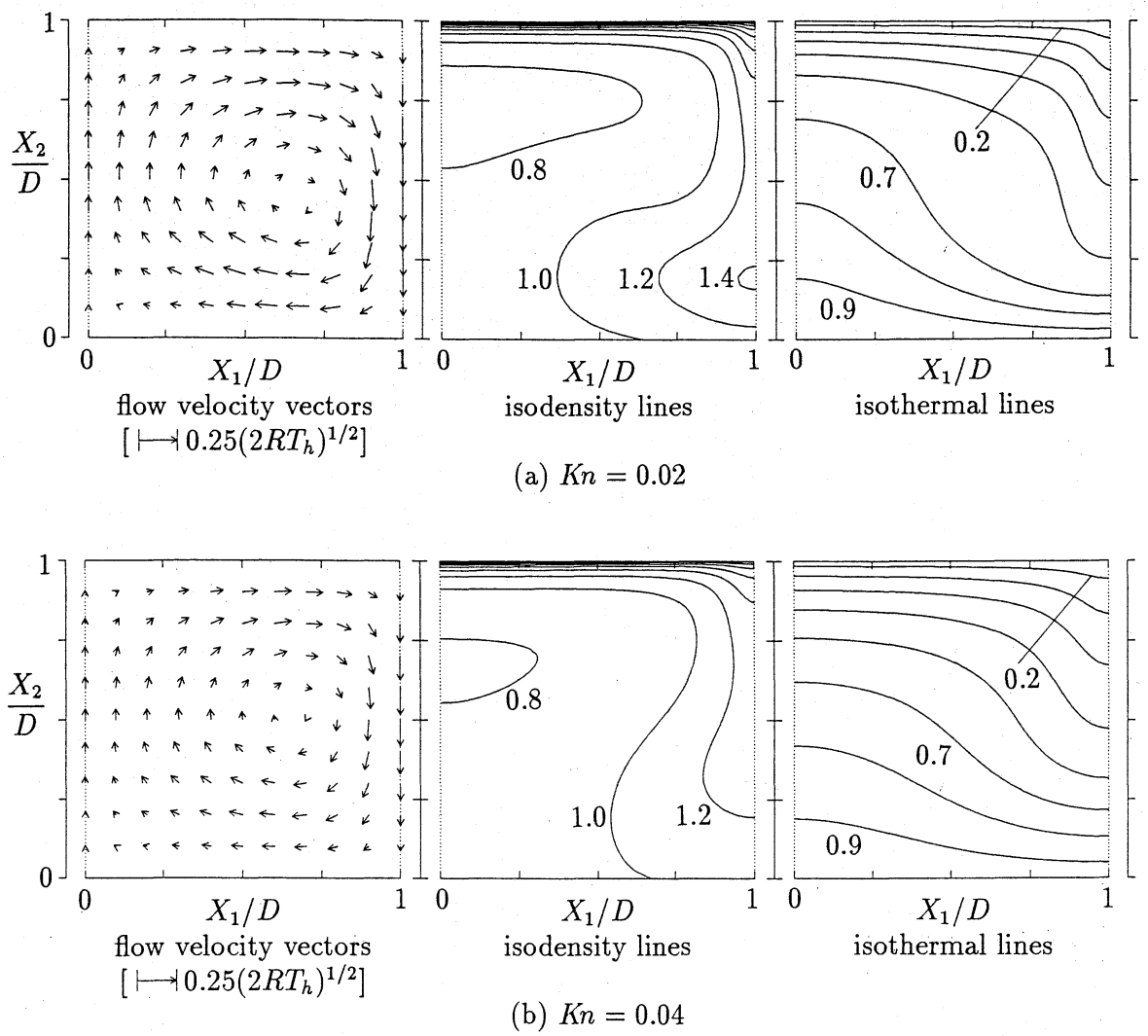

Fig. 5. Flow velocity vectors, isodensity lines, and isothermal lines for two Knudsen numbers, $Kn = 0.02$ and 0.04, with $L/D = 1$, $Fr = 3$, and $T_c/T_h = 0.1$. (a) $Kn = 0.02$ and (b) $Kn = 0.04$. The arrows indicate the velocity at their starting points. The contours $\rho/\rho_0 = 0.2n$ and $T/T_h = 0.1n$ are shown. [The (X_1, X_2) space is divided into 48×56 nonuniform rectangular lattices finer near the upper and right boundaries. The (ξ_1, ξ_2) space, limited to $|\xi_1|$ and $|\xi_2| \leq 4(2RT_h)^{1/2}$, is divided into 40×60 nonuniform rectangular lattices, finer near the lines $\xi_1 = 0$ and $\xi_2 = 0$.]

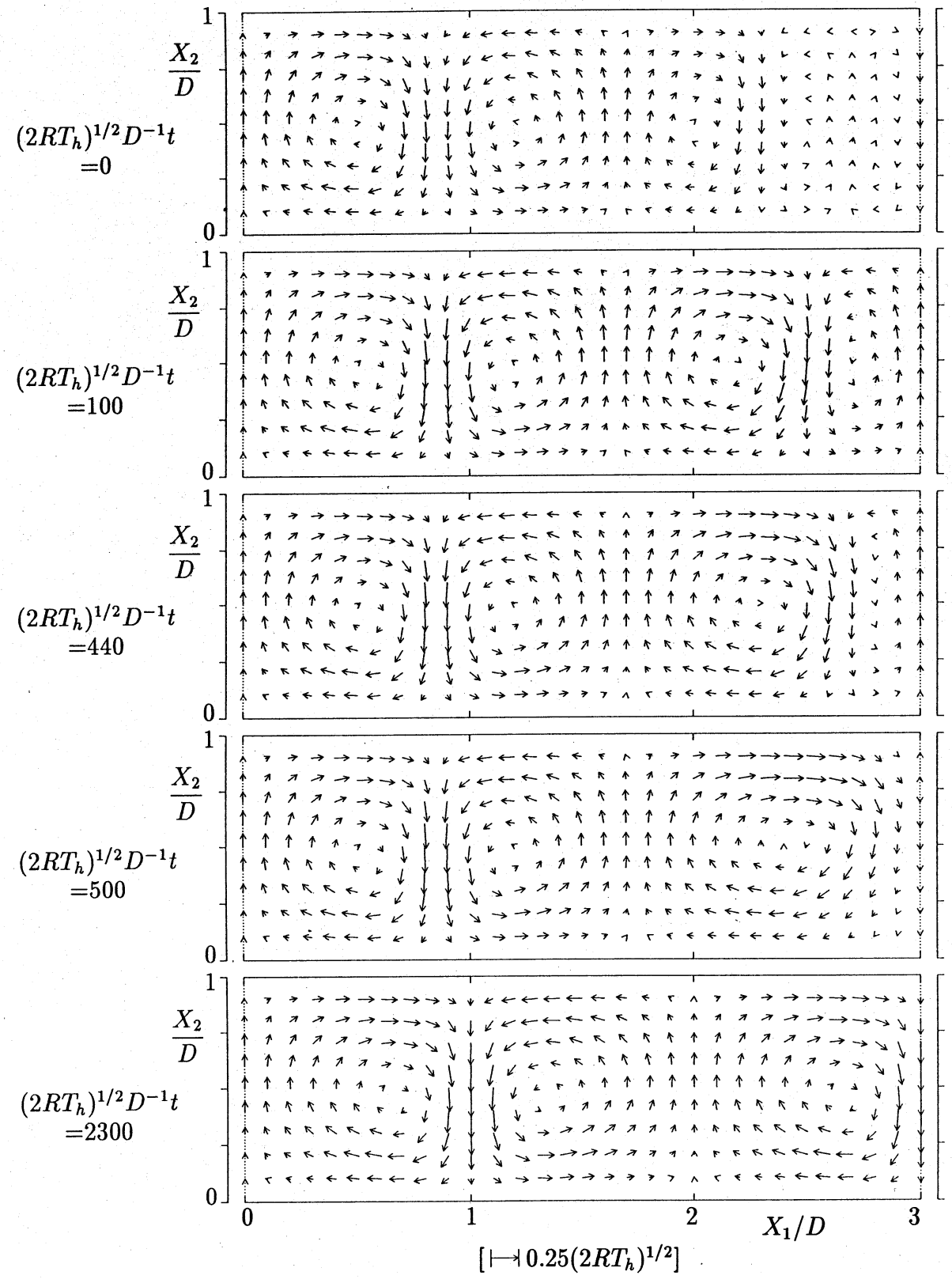

(a) $\alpha = 0.6$

Fig. 6. (See the next page for the caption.)

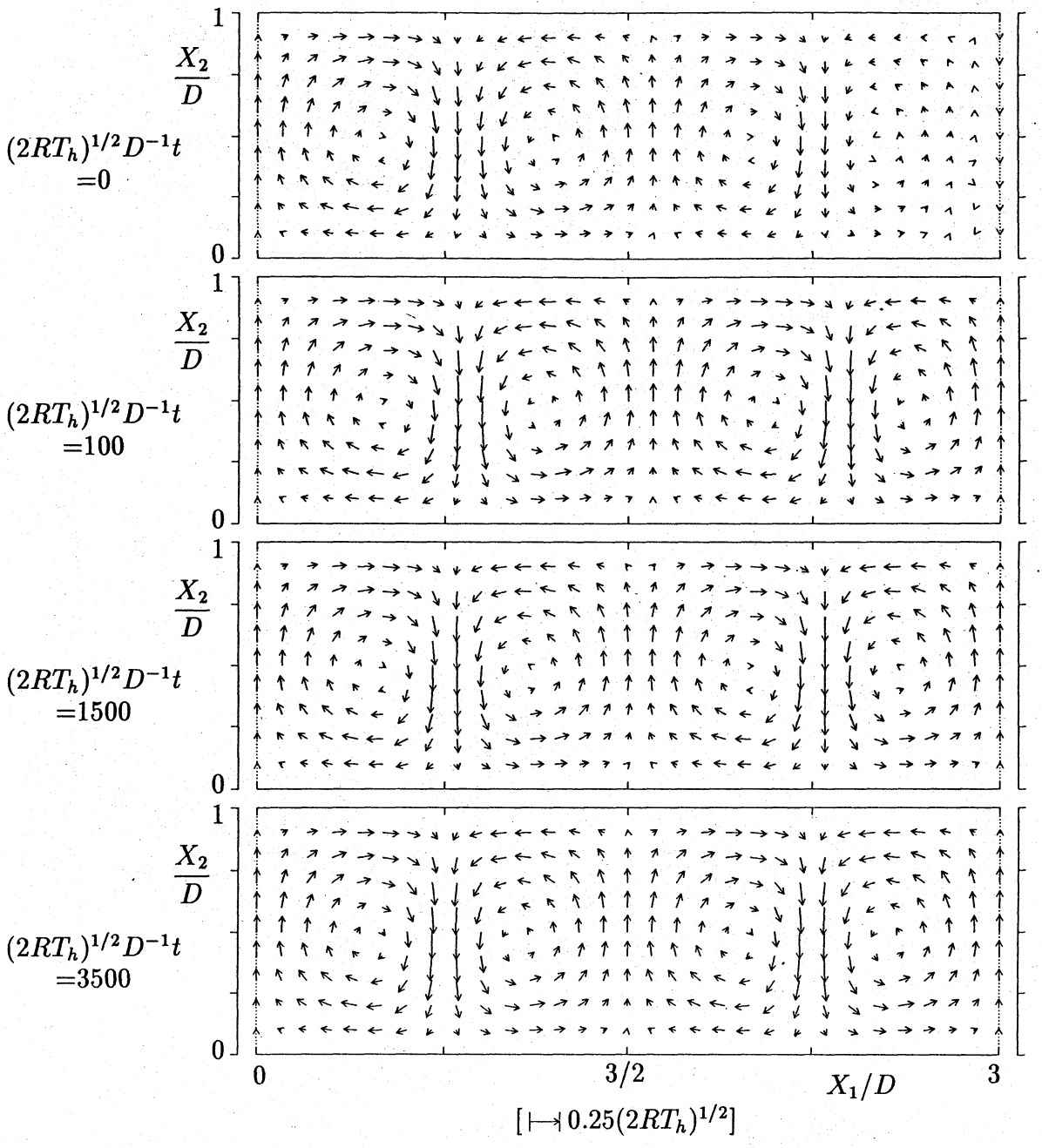

(b) $\alpha = 0.7$

Fig. 6. Bifurcation of flow for $L/D = 3$, $Kn = 0.02$, $Fr = 3$, and $T_c/T_h = 0.1$. (a) $\alpha = 0.6$ and (b) $\alpha = 0.7$. The time-development of velocity fields of the initial and boundary-value problem (1)–(8) with (10) is shown. The arrows indicate the velocity at their starting points. In (b) the most right "roll" is smallest at about $t(2RT_h)^{1/2}/D$ =50 $\sim$ 100. [The (X_1, X_2) space is divided into 96×28 rectangular lattices uniform in X_1 and nonuniform in X_2 (finer near the upper boundary). The (ξ_1, ξ_2) space, limited to $|\xi_1|$ and $|\xi_2| \leq 4(2RT_h)^{1/2}$, is divided into 40×40 nonuniform rectangular lattices, finer near the lines $\xi_1 = 0$ and $\xi_2 = 0$. The time step Δt is $\Delta t = 0.1D/(2RT_h)^{1/2}$. For accurate description of the initial stage, more detailed computation with a finer time step is required.]